Chapter 5. Discharging current-voltage characteristics of ferroelectric thin films

In this chapter, current–voltage(*J-V*) characteristics of ferroelectric thin films are studied by analyzing charging current characteristics. Possible electrical conduction mechanism is proposed to interpret the leakage current characteristics of the thin films.

5.1. ABSTRACT

Discharging current-poling voltage (J_D-V) characteristics were investigated in order to interpret the true leakage current-voltage (J_L-V) characteristics of ferroelectric thin films such as $Pb(Zr_{1-x}Ti_x)O_3$ (PZT) and $SrBi_2Ta_2O_9$ (SBT). Charging current-voltage (J_C-V) curves were measured by both step-sweep and step-pulse modes. The partial switching polarization current of FE thin film capacitors was observed in addition to non-switching polarization current that is equivalent to transient current at non-switching polarization states. A 'reverse step-pulse' technique was applied to eliminate partial switching effect, which determines both J_C-V and J_D-V at various temperatures. Based on the above observation, J_L -V curves were determined and modeled on the assumption that leakage current of FE thin film capacitors is controlled by Schottky emission.

5.2. INTRODUCTION

It is well known that $Pb(Zr,Ti)O_3$ (PZT) and $SrBi_2Ta_2O_9$ (SBT) thin films are typical NvFRAM material candidates. Electrical properties of those thin films, such as polarization-field (P-E) characteristics, imprint, and leakage current have been studied for several years. Many physical models describing the leakage current behaviors of ferroelectric films have been proposed and experimental data supporting these mechanisms have been presented. Schottky emission, space charge limited conduction (SCLC), Pool-Frenkel emission and ionic conduction were proposed for PZT thin films [1,2]. Only Schottky emission and SCLC were proposed for SBT thin films. Such a various experimental result and interpretation stems from several factors

including different measuring techniques and different electrode/ferroelectric interfaces such as interdiffusion layer, oxygen depletion layer and surface traps. Above all, conclusions based on *J-V* curve shape only can be ambiguous because in many cases different conduction mechanisms result in the similar *J-V* curves. In addition, it is difficult to directly measure leakage current of FE films. The current of the ferroelectric thin film capacitors under DC bias includes charging current (J_C) which consists of switching current (J_S) and transient current followed by the true leakage current (J_L). The transient current is essentially is equivalent to non-switching current. The aging effect (J_A) can influence the charging current, too. Hence, J_C is described as:

$$J_C = J_S + J_A + J_L \tag{1}$$

J_S disappears in much shorter time in comparison with other terms. J_A appears normally under high fields and/or at high temperature, which can be discriminated from the *J-time* curves. Therefore, J_C is mainly attributed to the sum of J_S and J_L. In general, it takes a long time to stabilize J_c to get true leakage current of the high dielectric materials. This dielectric relaxation (or soak time) is dependent on measuring techniques and prehistory of sample treatments such voltage bias and illumination. Recently, Stolichnov and Tagantsev asserted that the true leakage current of PZT thin films is time dependent because of the influence of injected charge entrapment during measurement [3]. However, no direct evidence was shown yet.

In this chapter, we attempted to acquire true leakage current of ferroelectric materials by excluding switching current component from the measured charging current. The discharging current, J_D, was utilized to interpret *J-V* curve. Two FE capacitors, $Pb(Zr_{0.53}Ti_{0.47})O_3$ (PZT53/47) and $SrBi_{2.1}Ta_2O_9$ (SBT) were selected as test capacitors. A 'reversed step-pulse' method was applied in order to eliminate switching current term and evaluate J_L correctly.

5.3. EXPERIMENT

PZT and SBT thin films were prepared onto platinized silicon wafer by the sol-gel and metal-organic decomposition (MOD) methods, respectively. The details of these film preparations are described elsewhere [4,5]. The thickness of all films was about 250 nm. Pt-top electrodes of $4x10^{-4}$ cm^2 area and 120-nm thickness were deposited by dc magnetron sputtering

method using shadow mask.

P-E hysterisis loop was measured using a RT66A standard ferroelectric tester (Radiant Technologies). Charging and discharging currents were measured using a electrometer/source (Keithley 617). The temperature dependence of these currents was measured using a programmable temperature controller. The measurement control and data acquisition were performed using self-made software. Two different methods were used for the study of *J-V* relations: (i) Staircase method and (ii) Reversed step-pulse method. In staircase method, the bias voltage was applied as a successive manner with delay time (t_d) of 300 sec, whereas the reversed step-pulse method utilizes pulsed bias signal with t_d of 10 sec and the bias voltage starts from 7V to 0.2V by applying –0.2 V bias.

5.4. RESULTS AND DISCUSSION

5.4.1. *Analysis of charging current*

Figure 5-1(a) shows the ferroelectric switching effect on *J-V* characteristics of SBT thin film capacitors. The capacitor was initially biased with – 5V followed by staircase application of bias up to + 5V. The observed current density showed negative differential resistivity at the voltage around 1V. Some of report has shown similar phenomenon, which explains the observed negative differential resistivity due to double injection of both electrons and holes into a ferroelectric film [1], a trap filling process [6] or an excess bismuth in SBT system [2]. However, we believe this phenomenon is more related with ferroelectric switching characteristics. The voltage which showed negative differential resistivity corresponds to the ferroelectric coercive voltage of the film, as shown in Fig. 5-1(b), in P-E hysterisis loop. In general, ferroelectric material can possess a partially polarized state without external field. In the presence of external electric field the partially polarized domain may draw additional charging current at the ferroelectric coercive voltage, hence, the resulting *J-V* curve may look having a negative differential resistivity. Watanabe *et al*. has also shown that the position of the dip also changes according to temperature. Because ferroelectric domain switching is a function of temperature the observed dip may appear at the lower voltages in *J-V* curve at the elevated temperatures.

Figure 5-2(a) shows the various components which contribute the measured charging

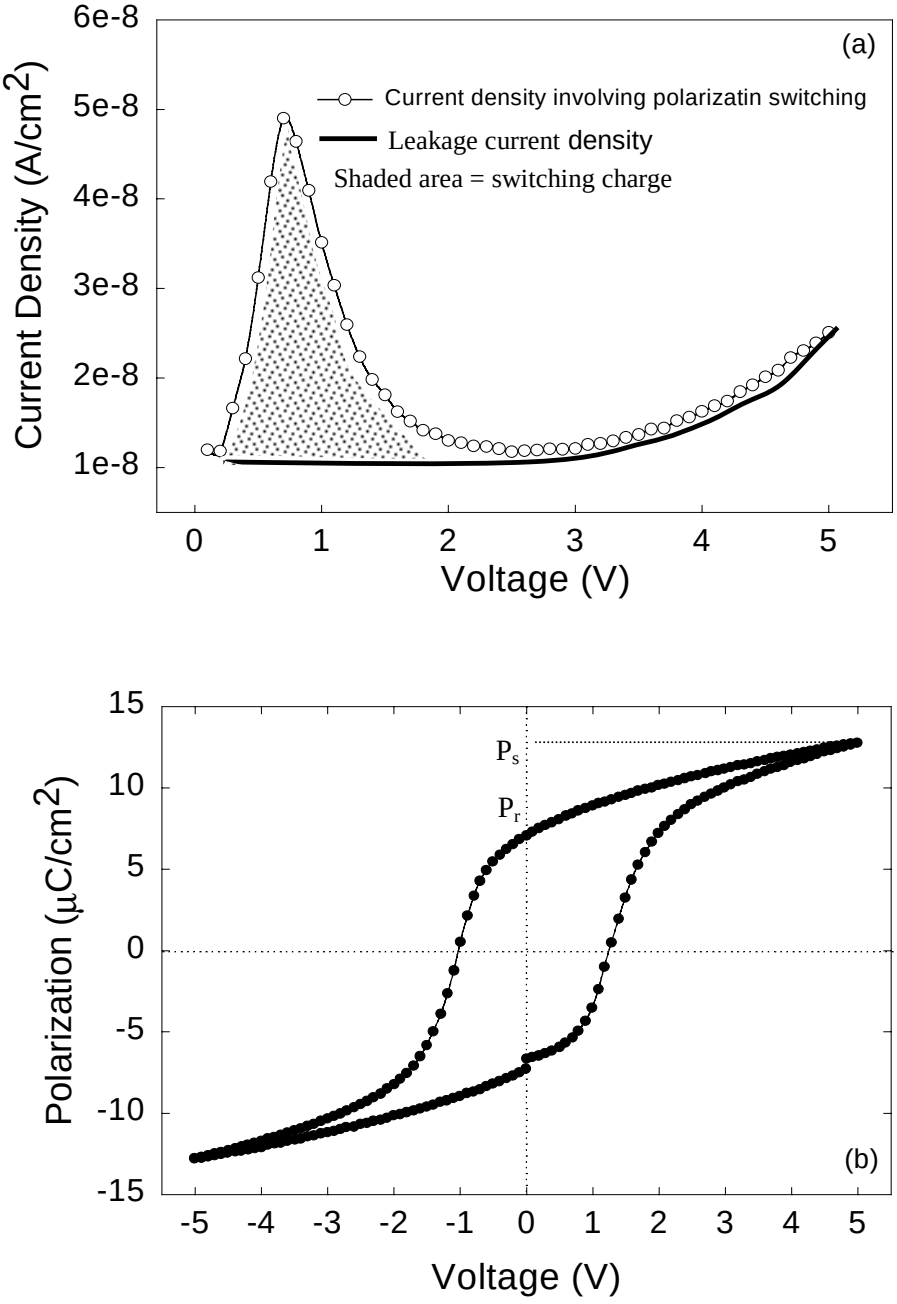

Figure 5-1. Effect of ferroelectric polarization on *J-V* curve

current. The charging current (J_C) usually consists of switching current (J_S) and leakage current (J_L) if measured near room temperature. The switching current, in turn, has two components in it;

$$J_S = J_{PS} + J_{NS} \tag{2}$$

J_{PS} denotes the current due to partial or full ferroelectric switching and J_{NS} is non-switching current which corresponds to dielectric relaxation phenomenon. Therefore, if we can remove J_{PS} from J_S, then, the J_S becomes the same with J_{NS}. One possible way to remove J_{PS} from J_S in ferroelectric charging current is applying bias from the voltage which makes a ferroelectric domains fully saturated, to lower bias voltages in backward manner as illustrated in Fig. 5-2(b). Once the ferroelectric domains become saturated then, the current will only reflect the charge between saturation polarization (P_S) and remanent polarization (P_r) in Fig. 5-1(b), which is expressed as non-switching current in the *J-V* curve. Therefore, the resulting J_C will become;

$$J_C = J_{NS} + J_L \tag{3}$$

In general, it takes a long time to stabilize J_C because of the dielectric relaxation phenomenon defined as the rate at which the dielectric polarization responds to a change of applied field in a material. The observed J_C is, usually, a combination of the dielectric relaxation current and true leakage current. Therefore, the estimation of the true leakage current is extremely difficult. Moreover, the domain wall motion which is accompanied by ferroelectric switching makes the relaxation process even prolonged [7]. For this reason, we have attempted interpret the J_C in terms of discharging current, J_D. The amount of charge generated by dielectric relaxation current (area A) will vanish within a certain time and, ideally, has to be the same with the charge by discharging current (area B) as illustrated in Fig. 5-3(a) [8]. Therefore, $J_{NS} \approx J_D$. The true leakage current in ferroelectric materials may be rewritten as;

$$J_L = J_C - J_D \tag{4}$$

In this chapter, we collected a current value with 10sec-delay time (t_d). The question is whether the 10-sec delay time is enough to measure true leakage current. To verify the charging current

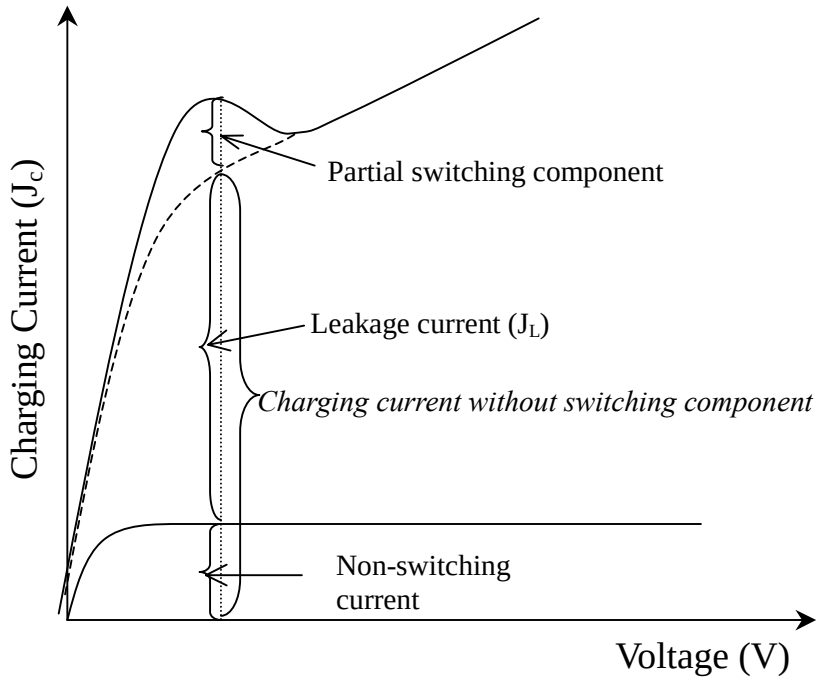

(a)

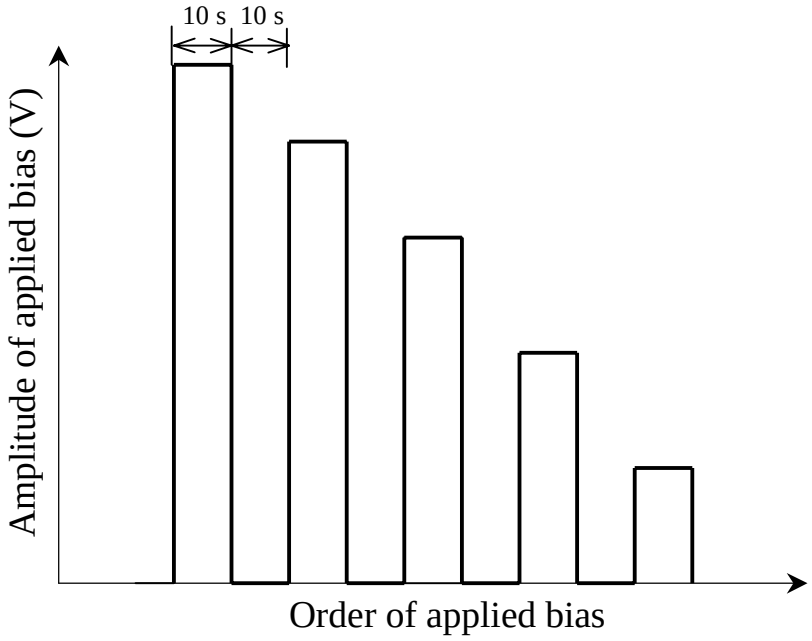

(b)

Figure. 5-2. Schematic view of (a) components contributing *J-V* characteristics and (b) reversed step pulse bias

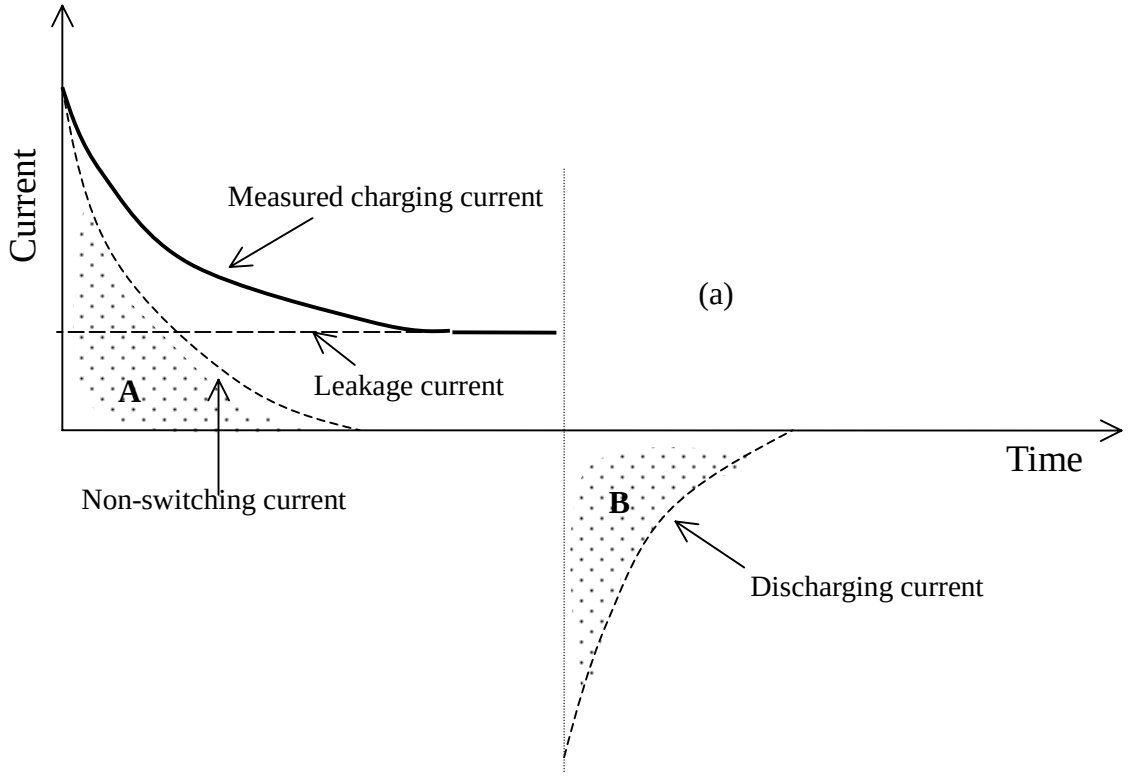

Figure. 5-3. (a) Schematic view of relationship between dielectric relaxation current and discharging current in *J-t* curve

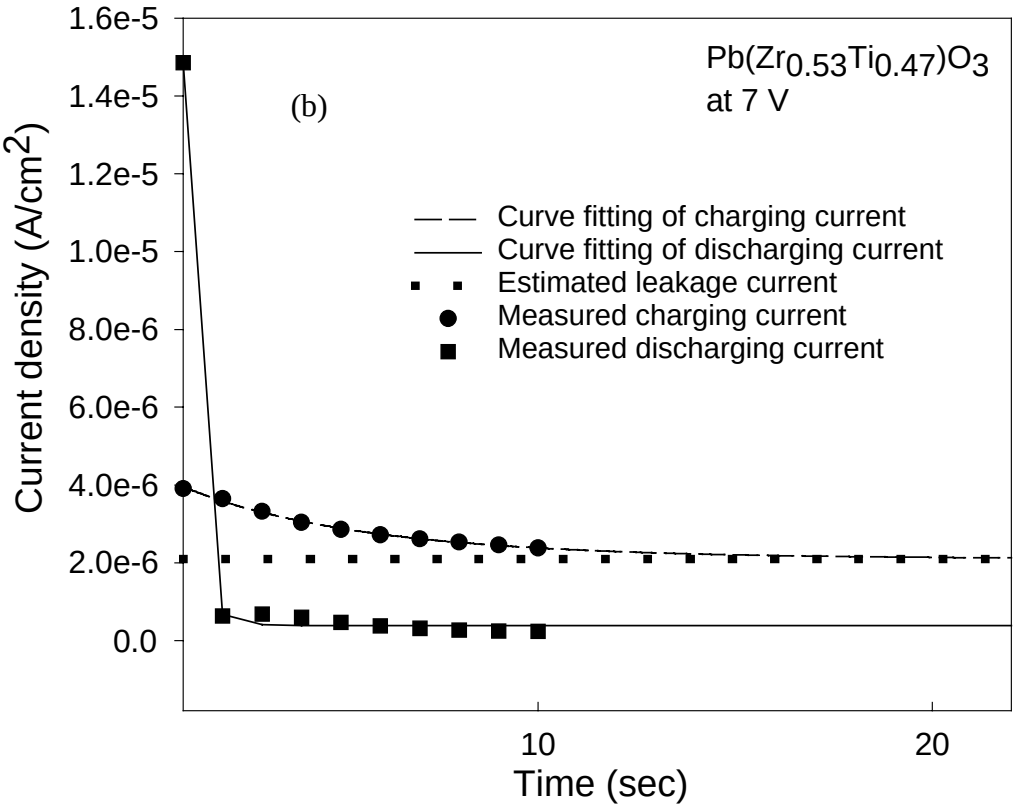

Figure 5-3 (b) *J-t* characteristics of PZT thin film at 7V

relationship with discharging current as a function of t_d, measured charging and discharging current in current-time (*J-t*) curve were mathematically fitted using the equation proposed by Yoo *et al*[9]. Firstly, the charging current was fitted with $J_C = a(1+bt)^{-n} + c$, where *a* and *b* denotes constants and *n* is a decay constant and *c* is an estimated true leakage current under steady state condition. The discharging current was also fitted using similar equation but, without the constant *c* because discharging current should decay to zero eventually. For valid conversion of discharging current to dielectric relaxation current the charge generated by dielectric relaxation has to be the same with the one by discharging current in a given delay time, t_d. Therefore,

$$\int_0^{t_d} [F(J_C) - c]dt = \int_0^{t_d} F(J_D)dt \qquad (5)$$

In this study, the current was measured with 10sec-delay time from 1 sec and the curve fitting was performed with 99.6% accuracy. The resulting calculated charge due to dielectric relaxation and discharging current were 7.3 μC/cm^2 and 6.1 μC/cm^2, respectively. The difference of 1.2 μC/cm^2 may arose from the time range between 0 to 1sec due to the limitation of the data acquisition software functionality.

Figure 5-4 (a) and (b) shows log J_C-V and log J_D-V characteristics of SBT and PZT thin films by reverse step-pulse measurement technique. Unlike in Fig. 5-1(a), no negative differential resistivity was observed. In the two different temperature regime, charging current of both films showed observable increase at 75 ^{o}C where as a negligible change was seen for the discharging current, which indicates that only the leakage current is a function of temperature. Therefore, from eq. (4), the interpretation of true leakage current using discharging current is valid at an elevated temperatures.

5.4.2. *Leakage current mechanism of ferroelectric thin film capacitors: ferroelectric Schottky emission*

Based on these discussion, we have investigated the conduction mechanism of J_L for PZT(53/47) and SBT capacitors. The most favored mechanism for leakage conduction of FE capacitors should be Schottky emission model, which describes the carrier injection through a

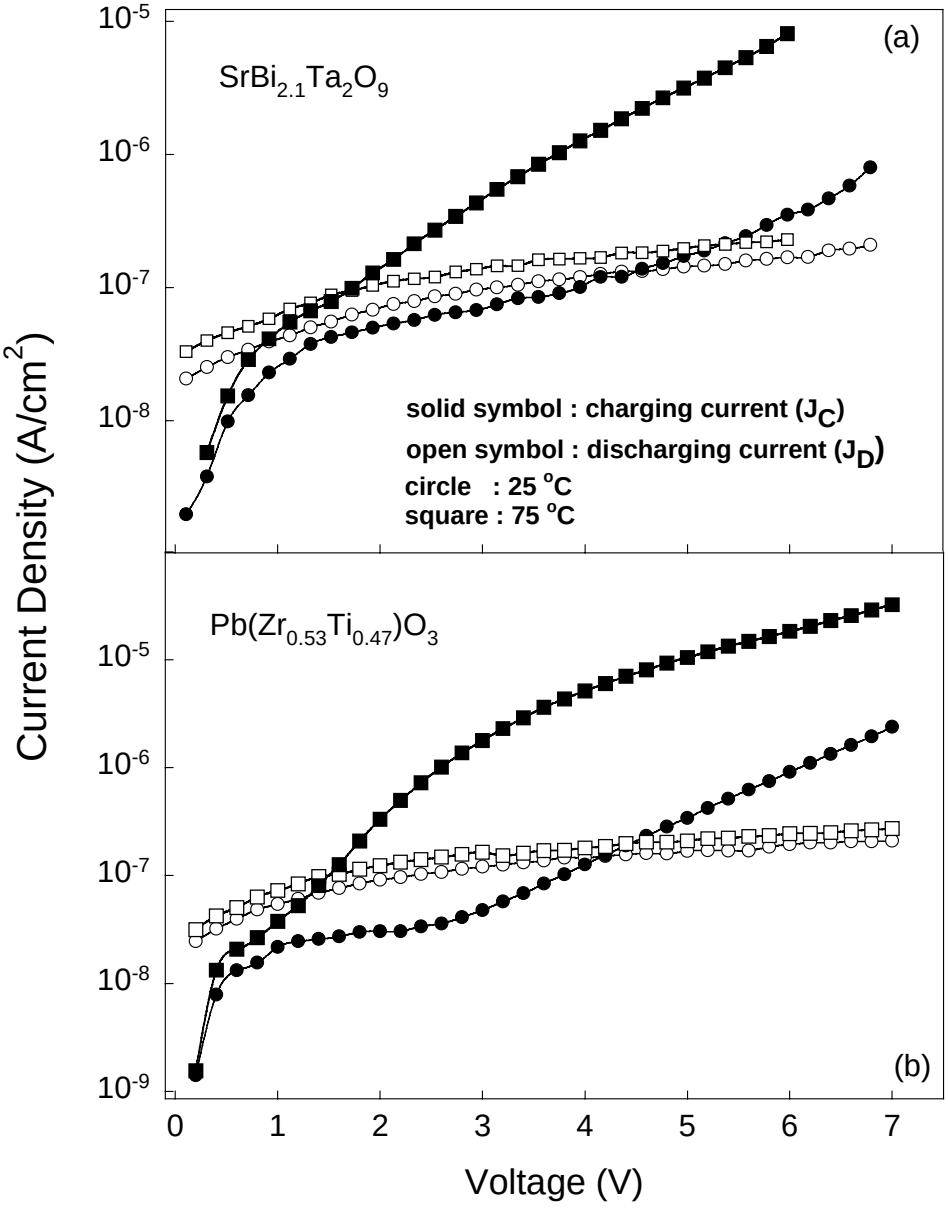

Figure. 5-4. J_C-V and J_D-V curves measured by means of 'reversed step-pulse' method at 25 °C and 75 °C in (a) PZT (b) $SrBi_{2.1}Ta_2O_9$ thin film capacitors.

blocking contact. Assuming leakage is controlled by the reverse-biased interface, the current for a Schottky diode is given by

$$J_L = A^* T^2 \exp(\frac{\alpha E^{1/2} - W_b}{k_B T}); \qquad \alpha = (\frac{q^3}{4\pi\varepsilon_0\varepsilon_r})^{1/2} \tag{6}$$

where A^* is the effective Richardson constant, which incorporates carrier mobility, k_B is the Boltzmann constant, T is temperature, W_b is the zero field barrier height, ε_r is the relative dielectric constant of the ferroelectric material, and ε_0 is the permittivity of free space. In order to check the agreement of experimental J_L-V curves with the Schottky-barrier model, we have adopted the same methods reported by Dietz *et al* [10]. In method (A), A^* is determined from the intercept of the $ln(J_L/T^2)$ *vs* $1/T$ plot at a given field. Then using A^* and the intercept of the $ln(J_L/T^2)$ *vs* $E^{1/2}$ plot at a given temperature, a barrier height is calculated. In method (B), α is determined from the slope of the $ln(J_L/T^2)$ *vs* $E^{1/2}$. The value of α is then taken with the slope of the $ln(J_L/T^2)$ *vs* $1/T$ curve to extract the barrier height.

Figure 5-5(a) and (b) show the plots of $ln(J_L/T^2)$ *vs* $1/T$ and $ln(J_L/T^2)$ *vs* $E^{1/2}$, respectively, for test capacitors of (a) PZT(53/47) and (b) SBT. Linear curve fitting was performed in the high temperature range above 323K and the high field range above 80 kV/cm for each plot. The barrier height (W_b) extracted from the above two methods are summarized in Table 5-1, where the values of W_b obtained from the two different analysis methods are consistent with each other. In the case of PZT, the calculated W_b turned out to be 1.01 eV which shows a little difference from the value reported by other groups. The difference may stem from the measuring techniques they used. The values of W_b for SBT as well as conduction mechanism are quite different from the result reported by Watanabe *et al*. Although they suggested SCLC dominated the high leakage conductivity of SBT including bismuth-excess specimens such contributions to the charging current of SBT are believed to be interpreted in terms of measuring technique.

5.5. CONCLUSIONS

In the present study we have showed the importance of measuring method to extract the

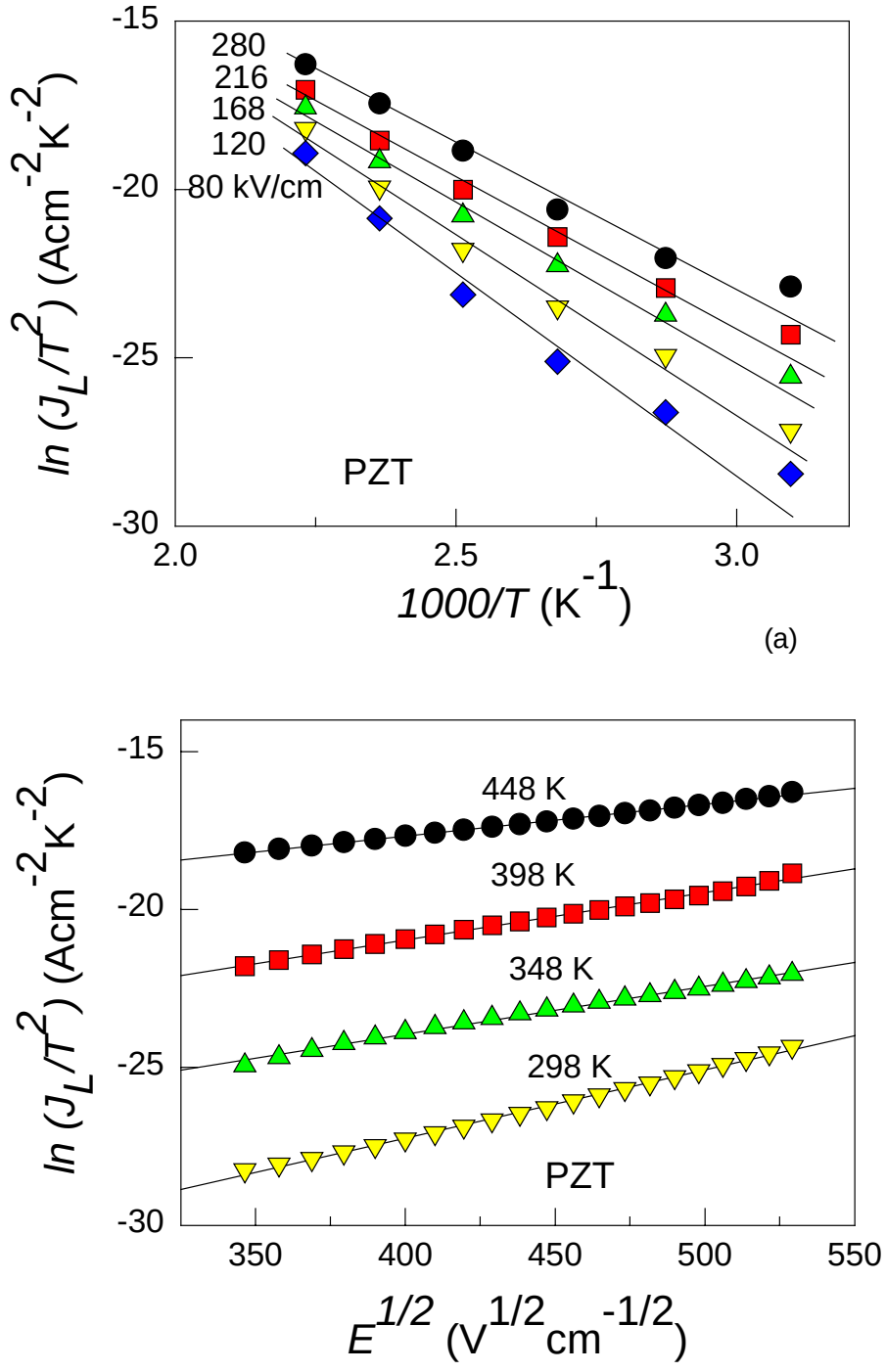

Figure. 5-5. Plots of $ln(J_L/T^2)$ *vs* $1/T$ and $ln(J_L/T^2)$ *vs* $E^{1/2}$ for test capacitors of (a) PZT

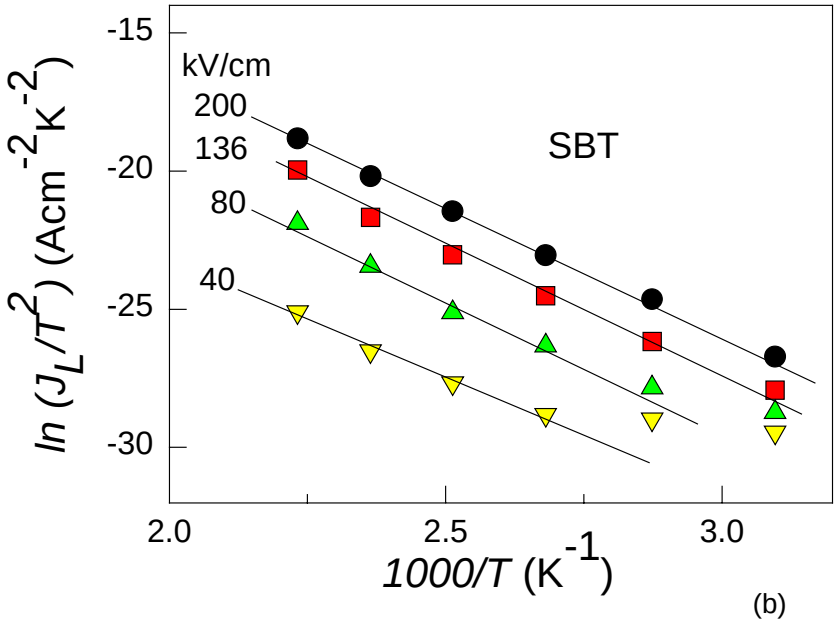

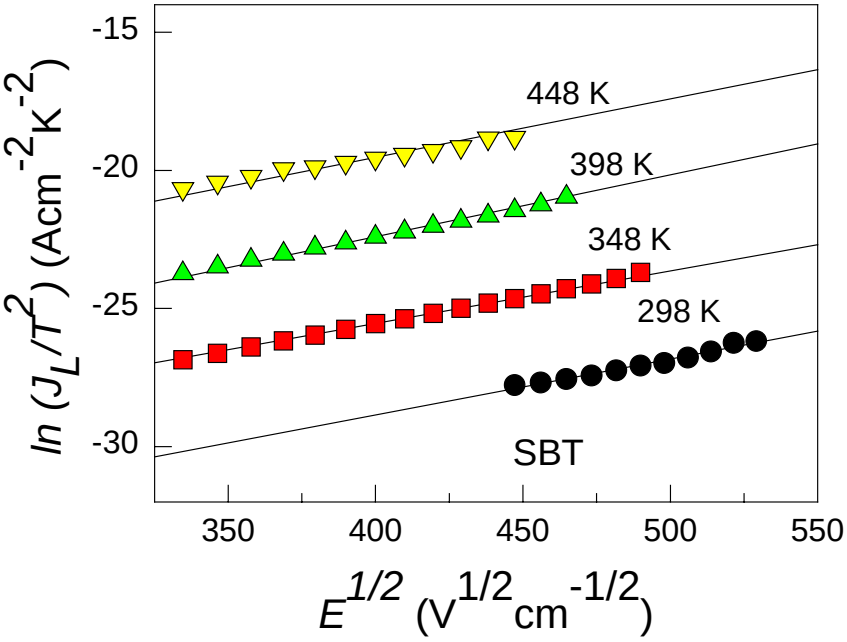

Figure 5-5 Plots of $ln(J_L/T^2)$ *vs* $1/T$ and $ln(J_L/T^2)$ *vs* $E^{1/2}$ for test capacitors of (b) SBT

Table 5-1. Barrier height (W_b) calculated for Schottky emission model. Here, the relative error in W_b is calculated with respect to the average value of W_b obtained at different temperature (method (A)) and field (method (B)).

	PZT (53/47)	SBT
W_b(eV) extracted from method (A)	1.01 ± 0.04	1.04 ± 0.06
W_b(eV) extracted from method (B)	1.01 ± 0.01	1.06 ± 0.01
$ln\,A^*$ in method (A)	3.5	1
α in method (B) in $eVcm^{1/2}/V^{1/2}$	4.76×10^{-4}	6.52×10^{-4}

true leakage current-voltage characteristics of ferroelectric thin film capacitors from the measured charging current-voltage curves. We found that the charging current-voltage curves measured by incremental voltage bias contains inevitable extrinsic effect due to the partially switched polarization, which was observed around the coercive voltage of the ferroelectric materials.

By applying reversed step-pulse bias we could remove the effect of partially switched polarization current and express the charging current in terms of non-switching polarization current (dielectric relaxation) and true leakage current. In addition, the discharging current, which is measured subsequently to the charging current, was successfully substituted for dielectric relaxation current in an effort to determine a true leakage current. By analyzing the discharging (J_D)-voltage characteristics we calculated the barrier heights for PZT(53/47) and SBT having Pt electrodes, which are determined as 1.01 eV and 1.05 eV, respectively. We believe that the measured charging current in ferroelectric thin film capacitors are basically dominated by the ferroelectric Schottky emission, especially at high field and/or high temperature.

5.6. REFERENCES

1. J.F. Scott, B.M. Melnick, J.D. Cuchiaro, R. Zuleeg, C.A. Paz de Araujo, L.D. McMillan, and M.C. Scott, Integr. Ferroelectr. **4**, 85 (1994)
2. K. Watanabe, A.J. Hartman, R.N. Lamb, and J.F. Scott, J. Appl. Phys. **84**, 2170 (1998)
3. I. Stolichnov and A. Tagantsev, J. Appl. Phys. **84**, 3216 (1998)
4. P.C. Joshi, S.O. Ryu, X. Zhang and S.B. Desu, Appl. Phys. Lett. **70**, 1080 (1997)
5. Y. Song, Y. Zhu, and S.B. Desu, Appl. Phys. Lett. **72**, 2686 (1998)
6. H.D. Chen, K.R. Udayakumar, K.K. Li, C.J. Gaskey and L.E. Cross, Integr. Ferroelectr. **15**, 89 (1997)
7. M.E. Lines and A.M. Glass, *Principles and applications of ferroelectrics and related materials* Clarendon Press, Oxford (1977)

8. R. Waser, NATO ASI Series, edited by O. Auciello and R. Waser (Kluwer, Dordrecht, 1995), Vol. 284, p. 223

9. In K. Yoo, Dissertation, Virginia Tech (1990)

10. G.W. Dietz, M. Schumacher, R. Waser, S.K. Streiffer, C. Basceri and A.I. Kingon, J. Appl. Phys. **82**, 2359 (1997)